8-10-2018

Hybrid Iterative Approach for Simulation of Radio-frequency Fields in Plasma

Vladimir A. Svidzinski
FAR-TECH, Inc.

Jin-Soo Kim
FAR-TECH, Inc.

Liangji Zhao
FAR-TECH, Inc.

S. A. Galkin
FAR-TECH, Inc.

Joseph Andrew Spencer
Utah State University

Recommended Citation
Physics of Plasmas 25, 082509 (2018); doi: 10.1063/1.5037110

Hybrid iterative approach for simulation of radio-frequency fields in plasma

V. A. Svidzinski, J. S. Kim, L. Zhao, S. A. Galkin, and J. A. Spencer

Citation: Physics of Plasmas **25**, 082509 (2018); doi: 10.1063/1.5037110
View online: https://doi.org/10.1063/1.5037110
View Table of Contents: http://aip.scitation.org/toc/php/25/8
Published by the American Institute of Physics

Hybrid iterative approach for simulation of radio-frequency fields in plasma

V. A. Svidzinski, J. S. Kim, L. Zhao, S. A. Galkin, and J. A. Spencer[a)]
FAR-TECH, Inc., San Diego, California 92121, USA

(Received 20 April 2018; accepted 20 July 2018; published online 10 August 2018)

A novel iterative approach for solving discretized linear wave equations in a frequency domain, which combines time evolution with iterative relaxation schemes, is presented. In this hybrid approach, each iteration cycle consists of evolution of electromagnetic (EM) fields in time over a specified number of field periods followed by several iterative relaxations. Provided that there is sufficient dissipation, both the time evolution and the iterative relaxations contribute to the convergence of the EM fields to the solution of the formulated full wave boundary value problem. Time evolution rapidly distributes EM fields, propagating with group velocity, over the simulation domain, while the iterative relaxations smooth the fields, reducing the numerical errors such that iteration cycles converge to a steady state solution, approximating the solution of the formulated problem. This approach is intended for large scale simulations which are beyond the capabilities of direct solvers presently used for solving wave equations in the frequency domain. The technique is demonstrated for solving wave equations on a regular grid using a cold plasma dielectric model with collisions for 2D modeling of EM fields in tokamak in an electron cyclotron frequency range. *Published by AIP Publishing*. https://doi.org/10.1063/1.5037110

I. INTRODUCTION

Accurate simulations of radio-frequency (RF) fields are very important for prediction of RF power deposition profiles and for modeling of antenna-plasma coupling in fusion and industrial plasma devices. Such simulations are needed for the analysis of the performance of the existing plasma devices using RF power and for helping in the design and optimization of the future devices.

Presently available advanced codes solving for full wave (without limiting approximation of small wavelengths relative to the size of the system) electromagnetic (EM) fields in plasma, which are driven by an antenna operating at fixed frequency ω, are using direct linear solvers for solving the discretized linear wave equations in a frequency domain. For hot fusion plasma applications, such codes include TORIC,[1,2] AORSA[3] (used for 2D Tokamak geometry), AORSA3D,[4] PSTELION[5] (developed for 3D Stellarator geometry), STELEC[6] [3D Stellarator electron cyclotron heating (ECH) modeling], and *FullWave*[7,8] (recently developed for 2D Tokamak geometry at FAR-TECH, Inc.). An approach in which the hot plasma response is added iteratively to the cold plasma model in the full wave simulations[9–12] has recently demonstrated its merits in practical simulations of some RF scenarios. This approach has also been relying on direct solvers for solving the underlying cold plasma wave equations.

The direct linear solvers [such as based on lower-upper (LU) decomposition] work well for wave equations, but their spatial resolution is limited due to the memory constraints in implementation of their algorithms. Due to this, the spatial resolution of such solvers even on supercomputing platforms is limited to an equivalent of approximately $\sim 10 \times 10^6$ grid points for a local (cold) plasma dielectric response model. This translates to a resolution of $\sim$100 wavelengths (in all directions) in a simulation domain in 2D geometry and $\sim$10 wavelengths in 3D. This resolution is significantly smaller when a fully nonlocal (all orders in the Larmor radius) hot plasma dielectric response model is used in wave equations.

While the available spatial resolution is sufficient for a number of practical applications, an accurate full wave modeling of many RF plasma scenarios is beyond the capabilities of the existing simulation tools, including the electron cyclotron resonance heating (ECRH) scenario in tokamaks and hot plasma RF modeling of 3D magnetic confinement configurations such as Stellarators and Torsatrons.

An effective iterative solver for discretized wave equations is required to increase the spatial resolution of the full wave simulations. The use of iterative solvers for wave equations is difficult because the resulting matrix is indefinite: the real part of the eigenvalues lies in both positive and negative half planes in the complex plane. Also, in many cases, the resulting matrix is ill-conditioned. The basic iterative methods such as Jacobi or Gauss-Seidel iterations in general do not converge for wave equations. For large problem sizes, only a few of the standard Krylov subspace iterative methods[13] demonstrate the convergence for wave equations [such as the least squares with QR factorization[14] (LSQR) and the generalized minimal residual method (GMRES)] but the convergence rate is impractically very slow. An effective preconditioning is required for Krylov subspace methods to become practical.

The development of effective preconditioning for solving a more simple Helmholtz equation is the subject of the ongoing research.[15] One of the most effective approaches is to use a shifted Laplacian preconditioner for this equation.[16,17] Vector wave equations in plasma, however, have a more complicated spectral structure due to the simultaneous presence of different wave branches. It becomes even more complex when the hot

[a)]Present address: Utah State University, Logan, UT 84322, USA.

plasma dispersion is included in the model. Formulation and implementation of the shifted Laplacian preconditioner to solve vector wave equations in plasma are a difficult task which is the subject of the ongoing research.

Due to similar reasons, the standard multigrid approach[18] is not effective for solving wave equations in large scale problems. One of the improvements to this approach for solving the discrete Helmholtz equation is done by enhancing the multigrid method by Krylov subspace iterations.[19] The application of multigrid methods to vector wave equations in plasma is the subject of the ongoing research. To the best of our knowledge, a practical iterative method for solving wave equations in plasma in large scale simulations is presently not available.

We developed a different iterative approach suitable for solving linear vector wave equations in a frequency domain in a dissipative medium. Our hybrid iterative approach combines time evolution with iterative relaxations. Each iteration cycle consists of evolution of EM fields in time over a specified number of field periods followed by several iterative relaxations. Time evolution part rapidly fills the simulation domain with a RF field propagating with group velocity, while the iterative relaxations smooth the intermediate solution and reduce numerical errors accumulated from time evolution. With sufficient dissipation of RF power in the model, both time evolution and iterative relaxations contribute to the convergence of the solution to the solution of the formulated boundary value problem. These time evolution-iterative relaxation cycles are repeated successively until an accurate solution is obtained. In most of the practical applications, the time evolution part makes a dominant contribution to the convergence of these hybrid iterations.

One should note that the time evolution approach by itself is often used to solve wave equations in a frequency domain by solving them as an initial value problem with the source terms oscillating with the antenna frequency. If the system is dissipative, the time integration could reach a steady state oscillating with the antenna frequency, approximating the sought solution of the frequency domain problem. The time integration uses much less memory than the direct solvers, and it can afford significantly larger grids. A finite difference time domain (FDTD) approach is often used to solve wave equations in a frequency domain in volumes containing dielectric materials,[20] and it is widely used to solve electrodynamic problems.[21]

For hot tokamak plasma with a nonlocal dielectric response, the use of the time evolution approach for solving linearized Vlasov-Maxwell's equations in a frequency domain was studied in Ref. 22. Fully kinetic time domain RF modeling of core plasma in fusion devices using particle in cell methods is still not practical due to limitations on the electron spatial and time scales. Nonlinear hybrid models with fully kinetic ions and drift kinetic electrons are starting to be used in fusion RF modeling.[23] Modeling of time evolution of RF fields in nonlinear fluid plasma models finds a number of applications in fusion plasmas, including modeling of an antenna near and far fields[24,25] in an ion cyclotron frequency range and modeling of propagation of a RF beam near the plasma edge in an ECR frequency range.[26]

It seems that the main limitation of using the time evolution approach for solving wave equations in a frequency domain is due to accumulation of numerical errors during the time integration. To be a "true" solution of the linear frequency domain problem, the time integration has to reach steady state oscillations with the antenna frequency. The question is whether a practical time domain simulation can integrate on a long enough time interval for the solution to reach steady state oscillations before the numerical errors become unacceptable. In fusion applications, the mode conversion processes and plasma resonances develop relatively slowly in time domain integration. In such cases, a steady state interference pattern is formed on a significantly longer time scale than the time of propagation of fast or slow waves through the simulation domain. Due to this reason, obtaining reliable steady state solutions by the time evolution alone is difficult in lower hybrid and electron cyclotron resonance (ECR) frequency ranges for realistic Tokamak parameters. To the best of our knowledge, the time evolution approach has not been used for solving wave equations in a frequency domain in a realistic Tokamak model in these scenarios.

In the present hybrid iterative approach, the errors in time evolution are reduced by the repetitive iterative relaxations such that the time evolution-iterative relaxation cycles converge to the solution corresponding to steady state oscillations. Thus, one can also consider this approach as "stabilization" of time integration, allowing for indefinitely long time integration until a steady state is reached.

We performed numerical tests of this approach for the cold plasma dielectric response model to solve for full wave RF fields in 2D Tokamak geometry for parameters relevant to the ECR frequency range current drive scenario in DIII-D. In our tests, explicit predictor-corrector time stepping is made, and iterative relaxations, minimizing the 2nd and the 4th order forms of residual, are applied. The results showed that the hybrid iterations are numerically stable and converge to the solution of the formulated problem provided that (1) the Courant stability condition is satisfied (in the examined cases, the time step is abided by the vacuum Courant condition); (2) a sufficient number of grid points are used to resolve the minimum wavelength; and (3) several iterative relaxations per cycle are made.

In this approach, the problem size is limited by memory required to store the sparse matrix of discretized wave equations in memory of a parallel cluster. For the considered cold plasma dielectric response model, the hybrid iterative approach was successfully tested on NERSC supercomputers using up to 1 B grid points in a simulation domain. This is approximately 100 times more grid points than the present practical limit of direct solvers for vector wave equations.

The approach is robust, and it is relatively simple to implement on parallel platforms. Its application for solving hot plasma wave equations is presently being investigated. In general, this approach requires more computing time to calculate the solution than the direct solvers based on LU decomposition. Also, when applied to the Helmholtz equation, we expect it to be slower than the advanced iterative approaches recently developed for this equation. The main area of the application of the hybrid iterative approach is for

solving wave problems which other methods cannot handle, in particular large scale full wave simulations in plasma. In addition, since this approach is much less restricted by computer memory, it could be the first choice for smaller computational systems. It also provides physics insights into how RF power propagates from an antenna, how the RF field fills the simulation domain, and how the steady state interference pattern is formed.

Implementation of the hybrid iterative approach for solving wave equations in plasma significantly extends the scope of RF modeling in fusion devices. With this technique, 3D full wave modeling of RF power in fusion devices becomes more practical. One of the important possible applications is full wave 3D modeling of RF beams on the adaptive grid in an ECR frequency range in tokamaks and stellarators.

In Sec. II general formulation of the hybrid iterative approach is presented. The results of numerical tests of the application of this approach for full wave modeling of RF fields in an ECR frequency range in tokamak are presented in Sec. III. Summary is made in Sec. IV

II. HYBRID ITERATIVE APPROACH FOR SOLVING WAVE EQUATIONS

We present the details of the hybrid iterative approach to solve linear wave equations in a frequency domain with specified boundary conditions. Wave equations are discretized in configuration space, and a local cold plasma dielectric response model is used. A similar approach can be applied for wave equations with a nonlocal hot plasma dielectric response model.[7]

The boundary problem is formulated from Maxwell's equations

$$\nabla \times \boldsymbol{E} = -\frac{1}{c}\frac{\partial \boldsymbol{B}}{\partial t}, \tag{1}$$

$$\nabla \times \boldsymbol{B} = \frac{4\pi}{c}(\boldsymbol{j} + \boldsymbol{j}_{ant}) + \frac{1}{c}\frac{\partial \boldsymbol{E}}{\partial t}, \tag{2}$$

assuming the time dependence proportional to $e^{-i\omega t}$ (ω is the driving frequency of the antenna). This results in wave equations in the frequency domain for complex amplitudes

$$\nabla \times \boldsymbol{E} = \frac{i\omega}{c}\boldsymbol{B}, \tag{3}$$

$$\nabla \times \boldsymbol{B} = \frac{4\pi}{c}[\hat{\sigma}(\omega, \boldsymbol{r})\boldsymbol{E} + \boldsymbol{j}_{ant}] - \frac{i\omega}{c}\boldsymbol{E}, \tag{4}$$

where $\boldsymbol{j}_{ant}(\boldsymbol{r})$ is the antenna current amplitude. The cold plasma conductivity tensor $\hat{\sigma}(\omega, \boldsymbol{r})$[27] is used in Eq. (4) to connect the complex amplitudes of RF plasma current and the electric field.

Equations (3) and (4), along with boundary conditions on the components of electric field amplitude at the boundaries of the simulation domain, formulate the boundary value problem (antenna problem) for wave equations in the frequency domain. These equations are discretized in configuration space on a grid of points or using finite elements to form a set of linear algebraic equations. The solution of the formulated linear equations approximates the solution of the antenna problem. In the present approach, these equations are solved iteratively by combining time evolution with iterative relaxations in each iteration cycle.

The time evolution for this approach is formulated as follows: we assume that components of electric and magnetic fields in Maxwell's equations (1) and (2) are complex functions of real t and $\boldsymbol{r}$. The source terms (antenna current) or boundary conditions (when sources are modeled at the boundary) in Eqs. (1) and (2) are assumed to be functions of the form $\boldsymbol{j}_{ant}(\boldsymbol{r})e^{-i\omega t}$ or $\boldsymbol{E}_b(\boldsymbol{r})e^{-i\omega t}$, where $\boldsymbol{E}_b$ is the complex amplitude corresponding to boundary conditions in Eqs. (3) and (4). We also assume that complex current in Eq. (2) is related to the complex electric field as

$$\boldsymbol{j}(t, \boldsymbol{r}) = \hat{\boldsymbol{\sigma}}(\omega, \boldsymbol{r})\boldsymbol{E}(t, \boldsymbol{r}). \tag{5}$$

Equations (1) and (2) with relation (5) are evolved in time numerically starting from an initial condition using the specified time-dependent source term or the boundary condition. The time dependence of $\boldsymbol{E}(t, \boldsymbol{r})$ and $\boldsymbol{B}(t, \boldsymbol{r})$ is predominantly oscillations with frequency ω with an additional frequency spectrum present due to the time transient of "turning on" the RF source, wave propagation in the simulation domain, and possible excitation of other eigenfrequencies (which dissipate in time) of these equations. If the medium is dissipative, the time integration will reach a steady state in which field components oscillate with frequency ω and thus have the form $\boldsymbol{E}(\boldsymbol{r})e^{-i\omega t}$, $\boldsymbol{B}(\boldsymbol{r})e^{-i\omega t}$. In such a steady state, the calculated complex amplitudes $\boldsymbol{E}(\boldsymbol{r})$, $\boldsymbol{B}(\boldsymbol{r})$ are the sought solution of the original full wave boundary value problem [Eqs. (3) and (4)].

In the time evolution formulation (1) and (2), the dielectric response (5) corresponds to the plasma response calculated for fixed ω, while in the physical time evolution of EM fields in plasma, the dielectric response corresponds to the excited spectrum of frequencies. Therefore, the calculated time evolution does not exactly correspond to the physical time evolution of the fields, but the converged solution is the solution of the formulated boundary value problem.

For the time evolution to converge to a steady state, the formulated equations must represent a dissipative system. We show that Eqs. (1), (2), and (5) represent a dissipative system if the original physical model is dissipative for perturbations oscillating at frequency ω. We analyze the energy relation for these equations, assuming that there are no sources in plasma ($\boldsymbol{j}_{ant} = 0$). Multiplying (1) by $\boldsymbol{B}^*$ and (2)* by $\boldsymbol{E}$ and summing the two together and integrating over a volume V, we obtain

$$\frac{1}{4\pi}\int_V d\boldsymbol{r}\left(\frac{\partial \boldsymbol{B}}{\partial t}\boldsymbol{B}^* + \frac{\partial \boldsymbol{E}^*}{\partial t}\boldsymbol{E}\right) = -\frac{c}{4\pi}\int_S d\boldsymbol{S}\boldsymbol{E}\times\boldsymbol{B}^* - \int_V d\boldsymbol{r}\boldsymbol{j}^*\boldsymbol{E}. \tag{6}$$

By assuming that volume V is limited by a superconducting shell, the surface integral in Eq. (6) disappears. By adding its complex conjugate to Eq. (6), we obtain

$$\frac{1}{4\pi}\frac{\partial}{\partial t}\int_V d\boldsymbol{r}(\boldsymbol{E}\boldsymbol{E}^* + \boldsymbol{B}\boldsymbol{B}^*) = -\int_V d\boldsymbol{r}(\boldsymbol{j}^*\boldsymbol{E} + \boldsymbol{j}\boldsymbol{E}^*). \tag{7}$$

Integral on the left hand side corresponds to the instantaneous electromagnetic energy. The time integration is expected to be stable if the time derivative on the left is negative, such that any perturbation decays in time. By using the relationship between conductivity and dielectric tensors, the right hand side can be written as

$$\boldsymbol{j}^*\boldsymbol{E}+\boldsymbol{j}\boldsymbol{E}^* = \frac{i\omega}{4\pi}\left[\varepsilon^*_{ij}(\omega,\boldsymbol{r})-\varepsilon_{ji}(\omega,\boldsymbol{r})\right]E_iE^*_j. \tag{8}$$

This expression is exactly the same as the equation for heat generated in unit volume per unit time in plasma in the monochromatic RF field having frequency ω and complex amplitude $\boldsymbol{E}$.[27] The right hand side of Eq. (8) is positive for any $\boldsymbol{E}$ if in the formulated plasma model oscillations with frequency ω dissipate their energy. This can be checked directly for the plasma model described by the cold plasma dielectric tensor. This shows that any initial perturbation in Eqs. (1), (2), and (5) will dissipate in time, such that if the RF field is driven by an external source, then the time evolution will eventually reach steady state oscillations. Equation (8) shows that the instantaneous energy of the electromagnetic field dissipates in time in the formulated equations for complex $\boldsymbol{E}$ and $\boldsymbol{B}$, while in the real physical system, a time averaged (over the wave period) EM energy dissipates in time.

In this time evolution formulation, the plasma response on the EM field is already included in the conductivity tensor (5), while it has to be calculated self-consistently in time evolution models based on fluid equations, such as those implemented in the fluid version of code VORPAL[28] and in code EMIT-3D,[26] used for solving wave propagation problems. These codes, however, can handle nonlinear wave plasma interaction problems while we are focusing on the linear plasma response. Our approach requires a pre-calculated plasma response on EM fields at a single frequency, making it technically simpler than the direct time integration of fluid equations. This is more pronounced when wave-plasma resonances are present in the simulation domain.

The formulated time evolution approach can be used to solve the antenna problem in plasma in a similar way as it is used to solve steady state electromagnetic penetration problems in dielectric or conducting volumes.[20] However, in general, it is much slower than the use of direct solvers since it usually requires a lot of RF cycles to reach a steady state interference pattern. This approach becomes very useful, however, for large scale problems when the direct solvers cannot handle the size of the problem due to memory constraints. For such large problems, the capabilities of the time evolution approach alone are in general limited due to accumulation of numerical errors, such that the time integration disintegrates before a steady state is reached.

In the present implementation of the approach, the time integration numerical errors are reduced after periods of time integration, and the solution is adjusted to the sought solution of the boundary value problem by applying minimization of the residual iterative relaxation method to discretized equations (3) and (4) and using the fields from time integration as the initial condition. The adjusted solution is then used as the initial condition to the next time integration period, and the time integration-iterative relaxation cycle is repeated. In general, the time integration has dominant contribution to the convergence of this scheme, while iterative relaxations mostly have a stabilizing effect. For large scale problems, the iterative relaxations alone converge impractically slowly and by themselves they cannot be used to solve the antenna problem. Thus, both components of this hybrid iteration scheme are crucial for its practical applications.

Minimization of the residual iterative relaxation method, used in our tests, is formulated as follows: Discretization of the boundary value problem, Eqs. (3) and (4), results in a set of linear equations

$$a_{ij}x_j = b_i, \tag{9}$$

where a_{ij} are elements of a square sparse matrix (i and j are its row and column indexes), x_j are elements of the vector of unknowns $\boldsymbol{x}$ (j is its row index), b_i are elements of the right hand side vector (i is its row index) whose nonzero elements correspond to the source terms and the boundary conditions, and the summation over the repeated index is assumed. Separation of real and imaginary parts of matrix elements and of the unknowns x_j is made in formulating equations (9), such that all elements in these equations are real numbers.

The residual of satisfying Eq. (9) is defined as

$$S = \sum_i (a_{ij}x_j - b_i)^n, \tag{10}$$

where n is an integer. In our tests, we considered values $n=2$ and 4. At each iterative relaxation, the residual is minimized along the straight line which passes through the initial guess point $\boldsymbol{x}_0$ in the direction of the gradient of S

$$x_i = \left.\frac{\partial S}{\partial x_i}\right|_{\boldsymbol{x}=\boldsymbol{x}_0}\tau + x_{0i}, \tag{11}$$

where i is the row index of vector $\boldsymbol{x}$, the variable τ parametrizes the straight line, and x_{0i} are the elements of the initial guess vector $\boldsymbol{x}_0$ (i is its row index). The calculation of $\partial S/\partial x_i$ involves matrix-vector multiplications. Substitution of Eq. (11) into Eq. (10) results in an equation for S as a polynomial in τ. For $n=2$, S is the quadratic polynomial in τ. Its minimum is found by a simple algebraic formula. For $n=4$, S is the 4th order polynomial in τ. Its minimum is found from the roots of the 3rd order polynomial $dS/d\tau$ which are calculated by the Lagrange method. The value of $\boldsymbol{x}$ along this straight line, corresponding to the value of τ, minimizing the residual S, is the updated unknown after one iterative relaxation (which is then used as a next initial guess). Such iterative relaxations smooth the solution, reduce numerical errors accumulated during the time evolution steps, and relax the solution towards the solution of the boundary value problem.

Our tests in an ECR frequency range showed that if there are enough grid points to resolve the minimum wavelength, if the Courant condition for the stability of explicit time stepping in vacuum is satisfied (the explicit predictor-corrector time integration scheme was used in our tests), and if a few ($\geq$2) iterative relaxations are made per each cycle, then this hybrid iterative procedure is numerically stable and

it converges to solution which is close to the solution of Eqs. (3) and (4).

The hybrid iterative approach presented here should be considered as a framework for solving linear wave equations in a frequency domain by this method. In this approach, each iteration cycle has two main steps. Step 1: Time evolution of Maxwell's equations (1) and (2), formulated for complex $\boldsymbol{E}$, $\boldsymbol{B}$ with plasma current defined by Eq. (5). This time evolution is performed on the time interval equal to a specified number of RF periods. Step 2: Iterative relaxation of solution, calculated in step 1, using the discretized form of wave equations formulated in a frequency domain [Eqs. (3) and (4)]. The solution from step 2 is then used as the initial condition in step 1, and the iteration cycles are repeated until the error of satisfying discretized equations (3) and (4) reduces to a specified value.

In our tests of this approach, we discretized Eqs. (1)–(4) on a uniform grid in configuration space using finite differences to approximate the spatial derivatives, and the time evolution was performed by a simple predictor-corrector method (see details in Sec. III). The iterative relaxations are performed by the above described minimization of the residual method applied to the discretized Eqs. (3) and (4). One could expect that other well-developed time evolution techniques or iterative relaxation methods, such as FDTD methods (explicit or implicit), the use of finite elements for spatial discretization both for time evolution and for iterative relaxation, and different Krylov subspace iterative methods, could be used in implementation of these steps.

In some cases, the convergence of the hybrid iterative approach can be improved by projecting the time evolution solution, calculated in step 1, on the time harmonic oscillating with frequency ω by taking integrals $\frac{1}{T}\int_0^T \boldsymbol{E}(t,\boldsymbol{r})e^{i\omega t}dt$, $\frac{1}{T}\int_0^T \boldsymbol{B}(t,\boldsymbol{r})e^{i\omega t}dt$ (T is the interval of time integration in step 1) and then use these harmonics as input to step 2. In certain cases, this results in convergence of the scheme even without dissipation in the model.

At lower frequencies, $\omega \ll \omega_{ce}$, the frequency spectrum of Eqs. (1), (2), and (5) contains high frequency oscillations (relative to ω) due to the effect of small electron inertia. To resolve these high frequencies in an explicit time stepping scheme, a significantly more restrictive time step (than the one abided by the vacuum Courant condition) is needed. In this case, an analog of the semi-implicit time integration approach, presented in Ref. 25 for the fluid plasma model, could be suitable for integrating Eqs. (1), (2), and (5). Another possibility to overcome this restriction on the time step is to modify Eqs. (1) and (2) by adding term $(\alpha/c)(\partial\boldsymbol{E}/\partial t + i\omega\boldsymbol{E})$ to Eq. (2) and term $(\beta/c)(\partial\boldsymbol{B}/\partial t + i\omega\boldsymbol{B})$ to Eq. (1) (α and β are the functions of spatial coordinates) which would not change the sought solution of the steady state oscillations. One could eliminate the high frequency part of the spectrum of Eqs. (1) and (2) by properly selecting functions α and β.

III. HIGH RESOLUTION MODELING OF THE ECRH SCENARIO IN TOKAMAK

We tested a hybrid iterative approach in 2D Tokamak-like geometry (assuming uniformity in the toroidal angle) for the cold plasma dielectric model, applicable when $\omega/k_\parallel v_T \gg 1$. The cold plasma model is rather accurate for ECH except near resonance or its harmonics. The cold plasma conductivity tensor, Eq. (5), depends on plasma density, magnetic field, and collision rates of plasma species.[27] The simulation domain is a square poloidal section of torus and coordinates R (along the major radius) and Z (vertical direction), $R_0 - a \le R \le R_0 + a$, $-a \le Z \le a$ (R_0 and a are the major and the minor radii of the torus). Conducting boundaries of the domain are assumed except at the location of the wave launcher. Equations (1), (2) and (3), (4) are converted to cylindrical coordinates R, ϕ (toroidal angle), Z, and ϕ—the dependence proportional to $e^{in_\phi\phi}$ is assumed, where n_ϕ is the toroidal mode number.

Equations are discretized on a uniform rectangular grid in R and Z coordinates, and simple central finite differences are used to approximate spatial derivatives in Eqs. (1) and (2) and in Eqs. (3) and (4) to the 2nd order accuracy in the grid step. Electric and magnetic field components are defined on the integer and on half-integer grid points correspondingly. Explicit predictor-corrector time stepping (2nd order approximation of the time derivative) is implemented for the time evolution of Eqs. (1), (2), and (5) in which $\boldsymbol{E}$, $\boldsymbol{B}$, and $\boldsymbol{j}$ are defined on the same time step. The same spatial grid is used in the time evolution and in the iterative relaxation parts. The applied time evolution algorithm is similar to the finite difference time domain solution of Maxwell's equation approach.[20] The numerical algorithm is parallelized by dividing the simulation domain between processors.

In results presented here, each iterative cycle consists of time evolution of Eqs. (1) and (2) [with $\boldsymbol{j}$ defined by Eq. (5)] for one RF field period followed by N_{it} relaxations, minimizing the 2nd order ($n=2$) residual in Eq. (10), and then followed by N_{it} relaxations, minimizing the 4th order ($n=4$) residual in Eq. (10). The results of the hybrid iterative approach are compared with the results obtained by using a direct solver to solve the discretized Eqs. (3) and (4). While the two solutions are slightly different for a given grid step, they both converge to the same solution of the formulated boundary value problem when the grid step approaches to zero.

The hybrid iterative approach is intended for solving large scale full wave problems which are beyond the capabilities of the available direct solvers. To show the capability of this approach, we present the results of full wave modeling of the ECRH scenario in plasma with realistic tokamak parameters. In general, such simulations require to resolve an ~500 wavelength in each direction in the poloidal section, which is beyond the limits of the direct solvers. We use reference parameters relevant to the DIII-D tokamak: $B_\phi = B_0 R/R_0$; $B_\theta = B_0[0.4(r/a) - 0.1(r/a)^2]$ (θ is the poloidal direction); $n_e = n_0[1.02 + \cos(\pi r/a)]/2$ for $r \le a$ and $n_e = 0.01 n_0$ for $r > a$ ($r = \sqrt{(R-R_0)^2 + Z^2}$ is the minor radius) with $B_0 = 2.2\,\mathrm{T}$, $n_0 = 10^{20}\ \mathrm{m}^{-3}$, $R_0 = 1.67$ m, and $a = 0.67$ m. Deuterium ions are assumed. These parameters correspond to the high electron density case in DIII-D, with $\omega_{pe}/\omega_{ce} \approx 1.5$ on the magnetic axis.

A wave launcher, with driving frequency $f = 110\,\mathrm{GHz}$, is designed for second harmonic heating and current drive.

We model it by specifying tangential components of the electric field at the boundary of the simulation domain. In our model, the launcher is placed at the upper right corner of the simulation domain (relevant to the outboard launch in DIII-D) with components E_R, E_ϕ, and E_Z, tangential to the boundary, specified at the boundary as being proportional to $\exp\{-[(R-R_0-a)\sin\theta_0/0.075a]^2\}\exp\{-[(Z-a)\cos\theta_0/0.075a]^2\}\exp(ik_R R+ik_Z Z)$. The coefficient of proportionality is $-\sin\theta_0$ for E_R, $\cos\theta_0$ for the E_Z component, and for E_ϕ, it is found from the condition $div(\hat{\varepsilon}\boldsymbol{E})=0$ at the corner. Wave numbers k_R and k_Z are found from the dispersion equation in vacuum (assuming small plasma density near the corner) $k_R^2+k_\phi^2+k_Z^2=\omega^2/c^2$ with $k_\phi=n_\phi/(R_0+a)$ and by specifying the launch angle θ_0 (with respect to R) of the RF beam in the poloidal section. We use reference value $n_\phi=1500$. Such an antenna launches the predominantly X-mode RF beam into plasma. The diameter of the launched wave front in the poloidal section approximately corresponds to the diameter of the RF beams ($\sim$10 cm) in DIII-D.

In this high density case, $\omega\approx\omega_{UH}=\sqrt{\omega_{pe}^2+\omega_{ce}^2}$ on the magnetic axis. The X-modes experience the cutoff near the plasma mid-radius, and they are reflected back to the wall,[29] while O-modes do not experience plasma resonances. Thus, these waves penetrate into the regions where the cold plasma model, used for their modeling, is rather accurate. To demonstrate the convergence properties of the hybrid iterative approach for different values of N_{it} and for better illustration of how the solution is formed, we first show the results of application of this approach for solving wave equations for scaled down plasma parameters by reducing B_0, ω, and n_ϕ by a factor of 10 and by reducing n_0 by a factor of 100. The rate of convergence of this scheme is sensitive to dissipation of waves in plasma. We use electron collision rate $\nu/\omega=0.01$ in the plasma, which is increased to $\nu/\omega=0.05$ near resonances. This collision rate corresponds to a relatively weak dissipation for the scaled down parameters, such that the launched waves are reflected several times from the conducting walls.

Simulations with these parameters and $\theta_0=60^\circ$ are performed on a server using $3000\times3000=9\times10^6$ grid points (total 54×10^6 of unknown field components) and 800 time steps per each RF period (iteration cycle). This number of time steps insures that the Courant stability condition is satisfied. Such a size of the problem approximately corresponds to the limit of capabilities of direct solvers. The convergence of the hybrid scheme is demonstrated in Fig. 1(a) which shows the dependence of relative error of satisfying Eqs. (3) and (4) (the maximum relative error of satisfying each equation) versus the number of iterative cycles N_c for different numbers of iterative relaxations N_{it} in each cycle. The antenna field amplitudes are turned on smoothly within one RF period starting from zero. Such initialization results in excitation of the dc component of the magnetic field, which satisfies Eqs. (1) and (2) but introduces an error to Eqs. (3) and (4). The dc component gradually relaxes to zero by iterative relaxations in each cycle, and it does not make significant influence on the results for $N_{it}\geq2$. For a better comparison of the results, the dc component is subtracted from the solution for the calculation of the error for $N_{it}=0$ and 1.

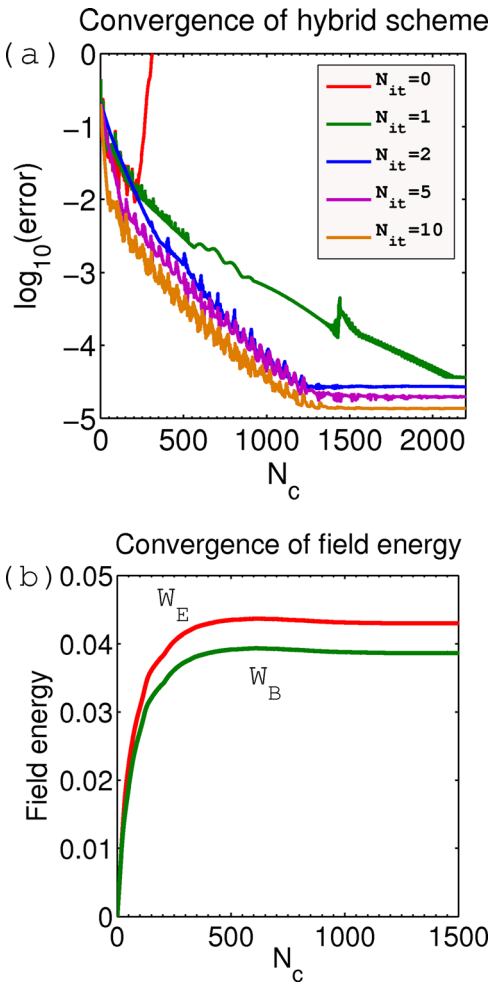

FIG. 1. Results for scaled down plasma parameters. (a) Convergence of the hybrid iterative scheme for different N_{it}. (b) Convergence of electric and magnetic energies for $N_{it}=5$.

For $N_{it}=0$ (time evolution only), the solution evolves for $N_c\sim200$ cycles after which it disintegrates due to accumulation of numerical errors. In this case, the time evolution does not reach the steady state, and the minimum error of satisfying Eqs. (3) and (4) is relatively large. For $N_{it}\geq1$, the iterations converge to a steady state in which the numerical errors accumulated during the time evolution periods are compensated by the subsequent iterative relaxations. The accuracy with which the steady state solution satisfies Eqs. (3) and (4) improves with the increase in the number of iterative relaxations N_{it} per cycle. However, for these parameters, this accuracy improves only marginally when $N_{it}\gtrsim5$. For a given grid size, the optimal value of N_{it} to get the better accuracy of the solution of the formulated boundary value problem is approximately in the range $2\lesssim N_{it}\lesssim10$. A more accurate solution would require the increase in the number of grid points rather than the increase in N_{it}.

Figure 1(b) shows the dependence of electric and magnetic energies, defined in Eq. (7), integrated over the simulation domain after iteration cycles versus N_c, calculated for $N_{it}=5$. These energies converge to constant values after $N_c\sim400$ cycles, indicating the convergence of the hybrid iterative scheme. These results show that the iterative relaxations, described by Eqs. (10) and (11), have smoothing stabilizing

effects on the time integration of wave equations. We also observed this effect directly by introducing some noise in the solution and then applying these relaxations. A similar convergence is also obtained by using iterative relaxations, minimizing the 2nd order residual [$n=2$ in Eq. (10)] only.

Formation of the steady state solution during this iterative procedure is shown in Figs. 2(a)–2(e) for the same scaled down plasma parameters corresponding to the result with $N_{it}=5$ in Fig. 1(a). These figures show the density plots of the real part of the E_Z component after different numbers of iterative cycles N_c. The RF beam is launched at angle 60° with respect to the R direction from the outboard side of the torus. Initially, it propagates approximately along a straight line in poloidal section experiencing diffraction [Fig. 2(a)]. Then, it reaches the region near the X-mode cutoff with a strong gradient of the index of refraction located at the plasma mid-radius, experiences refraction and scattering, and part of the beam gets reflected back in the outboard direction [Fig. 2(b)]. The reflected beam splits into several beams and reaches the conducting walls at $Z=-a$ and $R=R_0+a$ [Fig. 2(c)].

After several reflections from the walls, a steady state interference pattern starts to form [Fig. 2(d)]. The final steady state solution is shown in Fig. 2(e). The cutoff layer, shown in these figures, is calculated from the solutions of the cold plasma dispersion equation, assuming that the parallel wavenumber is defined by n_ϕ. The branch corresponding to the O-mode, having the electric field mostly parallel to equilibrium $\boldsymbol{B}$, does not experience a cutoff and propagates everywhere in the simulation domain. Component E_ϕ (not shown here), mostly corresponding to the O-mode, becomes comparable in magnitude to the E_Z component approximately half way to the cutoff region when the beam reaches denser plasma. This indicates that part of the beam converts from the predominantly X-mode in the antenna region to the O-mode in the core region. Figure 2(f) shows the plot of the power absorption profile $P_{abs}=\langle \boldsymbol{j}\cdot\boldsymbol{E}\rangle$ corresponding to the converged solution. In this case, nonresonant collisional damping has dominant contribution to the absorbed power.

Figures 3 and 4 show the results of solving wave equations by the hybrid iterative approach for the reference plasma parameters and for the same RF beam launch scenario ($\theta_0=60°$). The convergence of the hybrid scheme in this case is demonstrated in Fig. 3(a) which shows the dependence of relative error of satisfying Eqs. (3) and (4) versus the number of iterative cycles N_c for two different base electron collision rates $\nu/\omega=0.0025$ and $\nu/\omega=0.001$. In these cases, the collision rates are increased by a factor of 5 near the resonances, and increased collision rates in the low density plasma near the corners are used for a better convergence.

The simulations were performed on NERSC using $16\,000\times16\,000=256\times10^6$ grid points (~35 points per wavelength) and ran for $N_c\sim4000$ iterative cycles with $N_{it}=5$. The total number of Eq. (9) for the real and imaginary parts of field components corresponding to this grid size is ~3 B. Such a size of the problem is beyond the capabilities of direct solvers. For the larger collision rate (stronger beam absorption), the error of satisfying Eqs. (3) and (4) reached minimum after $N_c\sim1700$ iterative cycles after which it remained approximately constant. For the smaller collision rate, the error reached steady state minimum after $N_c\sim3500$ iterative cycles.

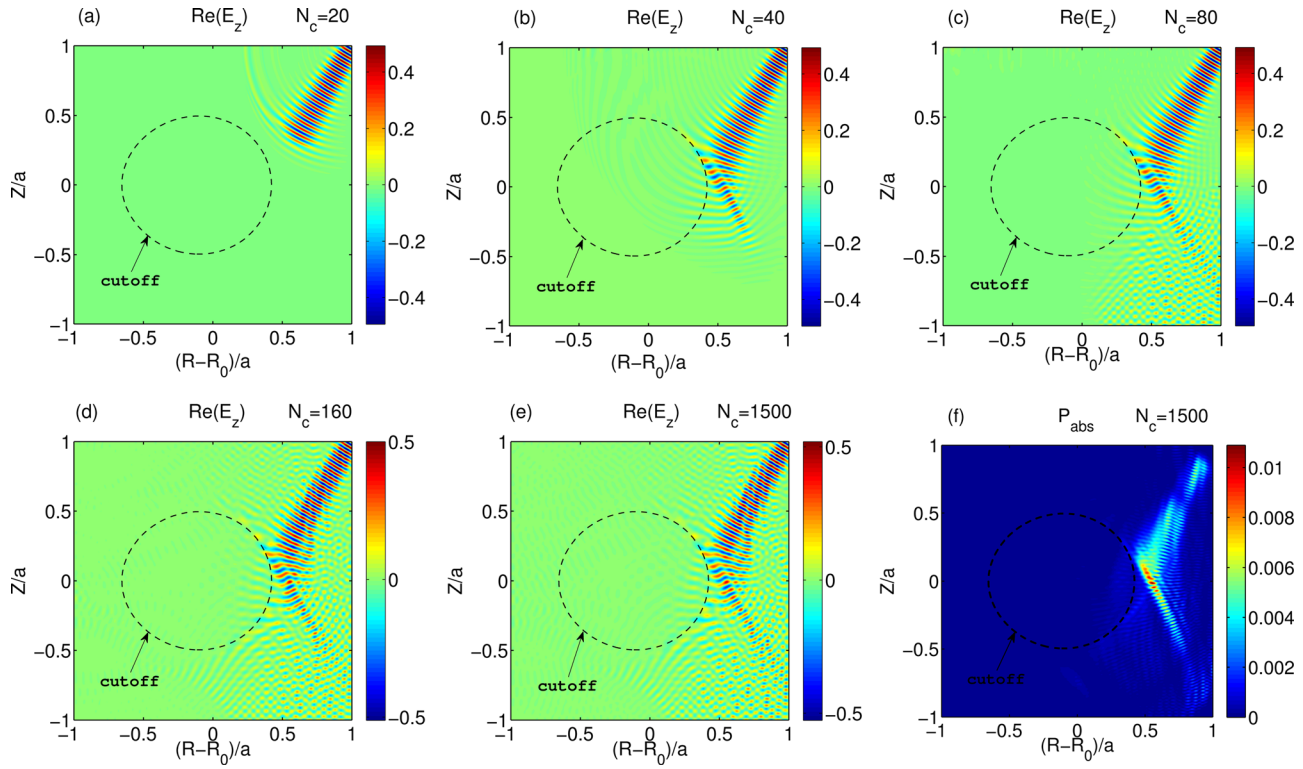

FIG. 2. Results for scaled down plasma parameters. (a)–(e) Formation of the solution. Profiles of Re(E_Z) in the poloidal section after N_c iterative cycles are shown. (f) Absorbed power profile for converged solution.

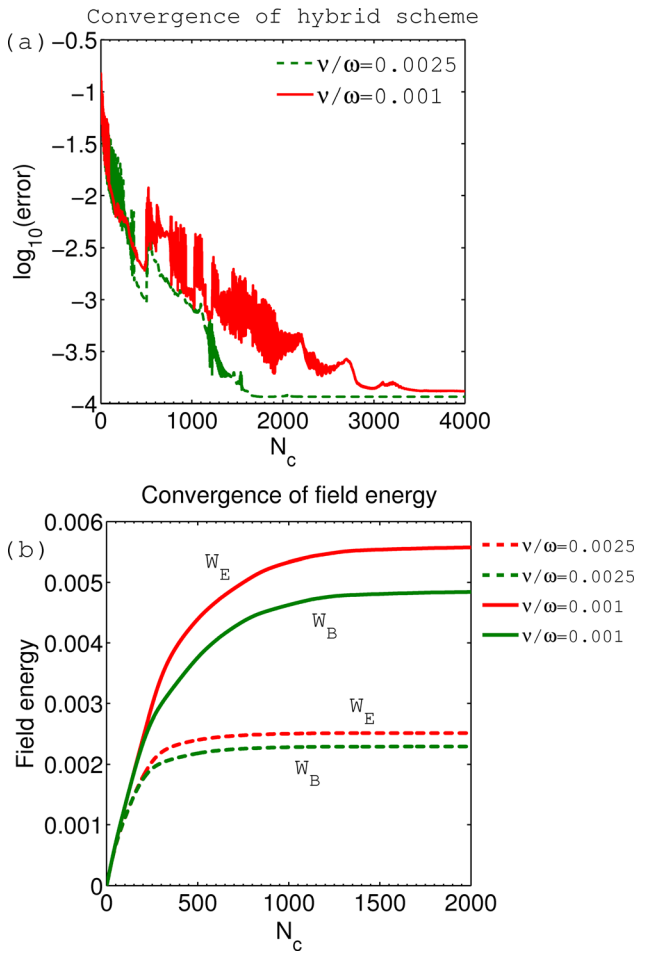

FIG. 3. (a) Convergence of the hybrid iterative scheme and (b) convergence of electric and magnetic energies for realistic tokamak plasma parameters for different ν/ω. The grid size in these simulations is $16\,000 \times 16\,000$.

Figure 3(b) shows the dependence of electric and magnetic energies of the RF field, integrated over the simulation domain after iteration cycles, versus N_c, for the two base collision rates. These energies converge to constant values. The convergence is faster in the case of stronger collisions. These results show that the hybrid iterative scheme is numerically stable and that it converges to a steady state solution which is close to the solution of the formulated boundary value problem. The convergence is faster for stronger dissipation in the model.

Different components of the converged solution, corresponding to $\nu/\omega = 0.001$, are shown in Fig. 4 along with X and O-mode ray trajectories calculated by a ray tracing code in the cold plasma model. The RF beam is launched as the predominantly X-mode at angle 60° with respect to R from the upper outboard corner of the simulation domain [see Figs. 4(a) and 4(b)]. Due to X and O mode coupling (mode conversion) for oblique propagation, the O-mode component is excited approximately half way to the cutoff region [see Fig. 4(c)]. The beam propagates as X and O mode components toward the X-mode cutoff region [Figs. 4(b) and 4(c)]. The two components interact with each other, mode converting multiple times along a substantial portion of the plasma minor radius. The X-mode component experiences stronger refraction near cutoff where the beam splits into two parts propagating as predominantly X and O mode components. After several reflections from the conducting walls, a steady state interference pattern is formed.

For these parameters, there is an ~400 wavelength within the diameter of the poloidal section. Figures 4(e) and 4(f) show the expanded view of area 1, showing more details of the wave structure. Most of the RF power is localized along the beam and its filaments, while a small fraction of the RF power scatters over a sizable fraction of the area of the simulation domain. RF power dissipates due to nonresonant collisional damping [Fig. 4(d)]. These high resolution full wave simulations allow us to focus on the details of the beam structure as it experiences multiple mode conversions between the X and O-modes and as it propagates through the region of the strong gradient of the index of refraction. To the best of our knowledge, no available advanced ray tracing code can model multiple mode conversions happening on such a long distance along the ray's trajectory (up to 100 wavelengths in this case). This is a very important physics result since the X-O mode conversion in the ECR range has a direct influence on the heating and current drive profiles in Tokamak experiments.

To better illustrate the high resolution capabilities of the hybrid iterative approach, in Fig. 5, we present the results corresponding to launching of a wide wave front from the vertical outboard boundary of the simulation domain. It is modeled by imposing boundary conditions $E_Z = 1$ and $E_\phi = 0$ at the boundary $R = R_0 + a$. The same plasma parameters, the wave frequency, and the grid size are used as in the previous result, except that $n_\phi = 0$ is assumed. In this case, the RF power penetrates most of the area of the simulation domain. To avoid strong excitation of surface wave modes, propagating between the electron cyclotron and upper hybrid frequencies,[30] which are excited along the horizontal boundaries in the inboard region for these parameters, a significantly increased collision rate in a small layer along the horizontal boundaries and the inboard vertical boundary is used.

The wave front, launched as a predominantly X-mode, propagates in the inboard direction and reaches the X-mode cutoff layer [see Fig. 5(a)]. The central part of the wave front, corresponding to $Z \approx 0$, reflects backward from the cutoff, while the peripheral parts of the front experience refraction in nonuniform plasma at different locations, forming a scattering pattern. The X-mode ray trajectories, launched in the horizontal direction from the vertical outboard boundary, are plotted in Fig. 5(a). The bright boundary layer, tangent to the cutoff layer at the outboard point of $Z = 0$, is the caustic surface (surface to which each of the rays is tangent) of this family of X-mode rays. The RF field intensity is accumulated at the caustic surface. This surface separates the region where the X-mode RF power mostly penetrates. This scattering pattern is somewhat similar to the results of scattering on cylindrical density filaments studied in Refs. 31 and 32. Surface wave structures are excited by the incoming wave near horizontal boundaries near $(R - R_0)/a = -0.6$. In other locations along the horizontal boundaries, a shadow layer is formed due to the enhanced dissipation rate there.

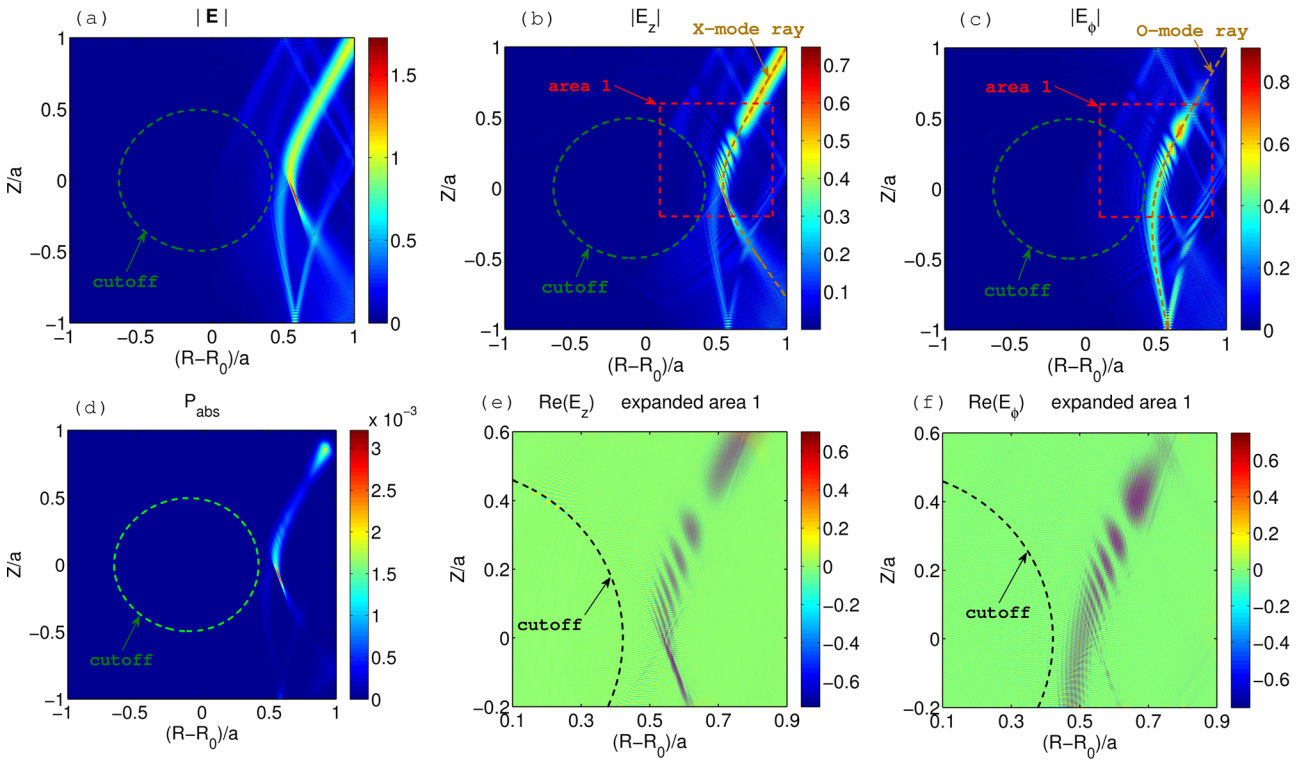

FIG. 4. Results for realistic Tokamak plasma parameters: profiles of (a) $|\boldsymbol{E}|$, (b) $|E_Z|$, and (c) $|E_\phi|$; (d) power absorption profile; (e) Re(E_Z) in area 1; and (f) Re(E_ϕ) in area 1. The grid size in these simulations is 16 000 × 16 000.

Figures 5(b) and 5(c) show field components Re(E_Z) and Re(E_ϕ) in the section of the simulation domain marked as area 1 in Fig. 5(a). Both these components have comparable amplitudes in this area, indicating that there is mode conversion between the X and O modes in the nonuniform plasma. The E_Z component does not penetrate much beyond the X-mode caustic surface, while the E_ϕ component does not experience the cutoff. The results in these figures show the fine resolution obtained by this technique as there are ∼60 wavelengths in each direction present inside the selected area 1. The convergence of the solution with the number of iterative cycles is similar to the previous case, shown in Fig. 3(a).

The high resolution results, presented here, are calculated with a simplified test version of the code, developed to study the formulated hybrid iterative approach. This code is not fully optimized for parallel performance. It utilized ∼100,000 cpu hours of computing resources to calculate these results at NERSC. The convergence of the approach was also tested at NERSC on grids having up to 1 B points.

A well-optimized full wave solver based on the presented hybrid iterative technique will be capable of handling 2D and 3D simulation domains with >1 B grid points in practical simulations of the cold plasma model on present supercomputers. This is approximately 100 times larger than the present practical limit of the direct solvers. The application of the hybrid iterative approach for solving wave equations in hot plasma is being investigated. The presented technique allows us to significantly extend the scope of full wave RF physics modeling.

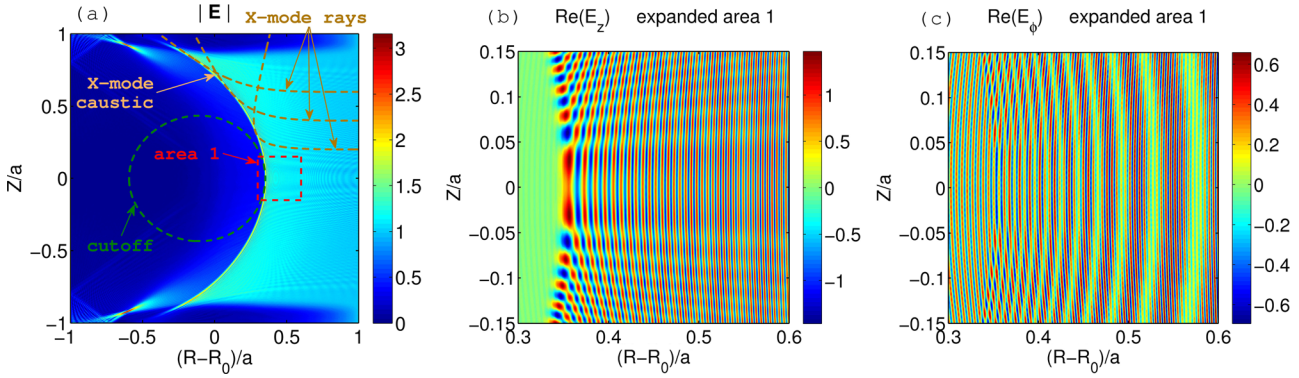

FIG. 5. Results for realistic Tokamak plasma parameters for a wide wave front launched from the outboard boundary: profiles of (a) $|\boldsymbol{E}|$, (b) Re(E_Z) in area 1, and (c) Re(E_ϕ) in area 1. The grid size in these simulations is 16 000 × 16 000.

IV. SUMMARY

A hybrid iterative approach for solving wave equations in a frequency domain which are discretized in configuration space is presented. The approach combines the time evolution technique with iterative relaxations, repeated successively. With sufficient dissipation of RF power in the model, the iterative cycles converge to a steady state solution which is close to the solution of the formulated boundary value problem. The time evolution mostly contributes to the convergence, while the iterative relaxations smooth the intermediate solution and reduce numerical errors accumulated from time evolution, stabilizing the iterative process.

The presented solution technique is suitable for large scale problems which cannot be solved by direct solvers due to the memory constraints or by the time evolution technique alone due to accumulation of numerical errors in the time integration. The hybrid iterative approach was successfully tested for solving wave equations with the cold plasma dielectric response model in 2D Tokamak geometry with plasma parameters corresponding to the realistic ECRH scenario. The convergence of the method with resolution up to 1B grid points is demonstrated at NERSC. This represents a significant increase in spatial resolution when compared with the application of direct solvers for similar problems.

Implementation of the hybrid iterative approach for solving wave equations in plasma significantly extends the scope of RF modeling in fusion devices. In particular, an accurate modeling of most mode conversion scenarios becomes possible. Its possible applications also include higher resolution modeling of RF fields in tokamaks and 3D full wave modeling of RF power in fusion devices including 3D modeling of RF beams in lower hybrid and ECR frequency ranges in tokamaks and stellarators.

ACKNOWLEDGMENTS

This work was supported by the DOE SBIR program under Grant No. DE-SC0011863.

This research used resources of the National Energy Research Scientific Computing Center, a DOE Office of Science User Facility supported by the Office of Science of the U.S. Department of Energy under Contract No. DE-AC02-05CH11231.

[1]M. Brambilla and T. Krücken, Nucl. Fusion **28**, 1813 (1988).
[2]M. Brambilla, AIP Conf. Proc. **403**, 257 (1997).
[3]E. F. Jaeger, L. A. Berry, E. D'Azevedo, D. B. Batchelor, and M. D. Carter, Phys. Plasmas **8**, 1573 (2001).
[4]E. F. Jaeger, L. A. Berry, E. D'Azevedo, D. B. Batchelor, M. D. Carter, K. F. White, and H. Weitzner, Phys. Plasmas **9**, 1873 (2002).
[5]V. L. Vdovin, "Development of scientific simulation 3D full wave ICRF code for stellarators and heating/CD scenarios development," Technical Report (RRC Kurchatov Institute, United States, 2005).
[6]V. L. Vdovin, Fusion Sci. Technol. **59**, 690 (2011).
[7]V. A. Svidzinski, J. S. Kim, J. A. Spencer, L. Zhao, S. A. Galkin, and E. G. Evstatiev, Phys. Plasmas **23**, 112101 (2016).
[8]V. A. Svidzinski, J. S. Kim, J. A. Spencer, L. Zhao, and A. Galkin, "Development of *FullWave*: Hot plasma RF simulation tool," paper presented at 59th Annual Meeting of the APS Division of Plasma Physics, Milwaukee, WI (2017).
[9]O. Meneghini, S. Shiraiwa, and R. Parker, Phys. Plasmas **16**, 090701 (2009).
[10]S. Shiraiwa, O. Meneghini, R. Parker, P. Bonoli, M. Garrett, M. C. Kaufman, J. C. Wright, and S. Wukitch, Phys. Plasmas **17**, 056119 (2010).
[11]D. L. Green and L. A. Berry, Comput. Phys. Commun. **185**, 736 (2014).
[12]P. Vallejos, T. Johnson, and T. Hellsten, EPJ Web Conf. **157**, 03059 (2017).
[13]Y. Saad, *Iterative Methods for Sparse Linear Systems* (SIAM, 2003).
[14]C. C. Paige and M. A. Saunders, ACM Trans. Math. Software **8**, 43 (1982).
[15]Y. A. Erlangga, Arch. Comput. Methods Eng. **15**, 37 (2008).
[16]A. Bayliss, C. I. Goldstein, and E. Turkel, J. Comput. Phys. **49**, 443 (1983).
[17]Y. A. Erlangga, C. Vuik, and C. W. Oosterlee, Appl. Numer. Math. **56**, 648 (2006).
[18]U. Trottenberg, C. Oosterlee, and A. Schuller, *Multigrid* (Academic Press, 2000).
[19]H. C. Elman, O. G. Ernst, and D. P. O'Leary, SIAM J. Sci. Comput. **23**, 1291 (2001).
[20]A. Taflove, IEEE Trans. Electromagn. Compat. **EMC-22**, 191 (1980).
[21]A. Taflove and S. C. Hagness, *Computational Electrodynamics: The Finite-Difference Time-Domain Method* (Artech House, Inc., Boston, 2005).
[22]V. A. Svidzinski and D. G. Swanson, Phys. Plasmas **8**, 463 (2001).
[23]J. Bao, Z. Lin, A. Kuley, and Z. X. Lu, Plasma Phys. Controlled Fusion **56**, 095020 (2014).
[24]T. G. Jenkins and D. N. Smithe, EPJ Web Conf. **157**, 03021 (2017).
[25]D. N. Smithe, Phys. Plasmas **14**, 056104 (2007).
[26]M. B. Thomas, M. W. Brookman, M. E. Austin, A. Kohn, R. J. La Haye, J. B. Leddy, R. G. L. Vann, and Z. Yan, "Resolving ECRH deposition broadening due to edge turbulence in DIII-D by 3D full-wave simulations," preprint arXiv:1710.03028v1 (2017).
[27]D. G. Swanson, *Plasma Waves* (Academic Press, Inc., San Diego, CA, 1989).
[28]C. Nieter and J. R. Cary, J. Comput. Phys. **196**, 448 (2004).
[29]M. Cengher, J. Lohr, Y. Gorelov, A. Torrezan, D. Ponce, X. Chen, and C. Moeller, IEEE Trans. Plasma Sci. **44**, 3465 (2016).
[30]A. W. Trivelpiece and R. W. Gould, J. Appl. Phys. **30**, 1784 (1959).
[31]A. K. Ram and K. Hizanidis, Phys. Plasmas **23**, 022504 (2016).
[32]Z. C. Ioannidis, A. K. Ram, K. Hizanidis, and I. G. Tigelis, Phys. Plasmas **24**, 102115 (2017).